Photino Hypothesis II: Field-Theoretic Reconstruction of Light and the Unified Mechanism of Its Phenomena

Tuahua Chen
(Independent Researcher, Guilin, China)
Corresponding Author: Tuahua Chen E-mail: 574581920@qq.com

Abstract

The wave-particle duality of light and its origin are central challenges in modern physics. As the second paper in the "Photino Hypothesis" series, this paper proposes a photino field excitation theory for electromagnetic waves, based on the space-time medium framework established in Hypothesis I [1]. **This theory interprets the photon as a quantized excitation mode of the space-time substrate (the photino field)**. Its energy $E_\gamma = h\nu$ and equivalent mass $m_\gamma = E_\gamma/c_0^2$ both originate from the dynamic interaction between electron vibrations and the photino field. The theory shows that the constancy of the speed of light $c_0 = \sqrt{\alpha s/2}$ is a natural consequence of the local homogeneity of the photino field, thereby providing a microscopic interpretation for the vacuum permittivity $\varepsilon_0$and permeability μ_0. Based on the intrinsic relationship between photon properties and photino field density （$\nu, m_\gamma \propto \sigma_{pe}(r)$, this theory establishes a unified framework for explaining redshift phenomena: it accurately describes the gravitational enhancement effect of compact matter by introducing a β correction factor, and proposes a photon fatigue model $z = e^{\alpha D} - 1$ as a new mechanism for cosmological redshift. This framework successfully derives the hydrogen atomic spectrum, accurately describes the gravitational deflection of light $\left(\alpha = 4GM/\left(c_0^2 r\right)\right)$, and shows high consistency with observational data from various types of celestial objects. Furthermore, the theory provides a novel physical explanation for the Cosmic Microwave Background (CMB), attributing its black-body spectral distribution to the thermal statistical properties of quantum fluctuations in the photino field. This theory not only offers a field-theoretic ontological explanation for wave-particle duality but also unifies the wave and particle nature of light within the excitation picture of the space-time medium, establishing a self-consistent theoretical foundation for understanding optical phenomena from the microscopic to the cosmic scale. **Subsequent papers in this series will explore the field-theoretic reconstruction mechanisms for magnetism, neutrinos, and the strong interaction, respectively**.

Keywords: Photino; Photon Essence; Quantized Excitation; Constancy of Light Speed; Unified Field Theory of Redshift; Photon Fatigue Effect

1 Introduction

The quest to understand the nature of light has permeated the history of physics. From Newton's corpuscular theory and Huygens' wave theory, to Maxwell's electromagnetic theory, and

then to Einstein's light quantum hypothesis, human understanding has oscillated between wave and particle pictures. Although quantum electrodynamics (QED) formally bridges this contradiction through second quantization, the physical origins of the photon's fundamental properties—such as the mechanism for its zero rest mass, the origin of the constancy of the speed of light, and a unified field-theoretic description of redshift phenomena — remain profound and unresolved issues.

Photino Hypothesis I[1] successfully reconstructed the microscopic mechanism of gravity within a novel framework of a space-time medium. This paper aims to extend this framework into the realm of electromagnetic waves, specifically addressing the fundamental question of the nature of light. The core idea is to reinterpret the photon as a quantized excitation of the photino field, thereby providing a field-excitation-based physical ontological explanation for wave-particle duality. The main advances of this theory include:

1. **Field-Theoretic Origin of Photon Properties:** Deriving the energy-frequency-dynamic mass relationship of the photon naturally from the interaction between electron vibrations and the photino field.
2. **Medium Interpretation of Light Speed Constancy:** Reducing the constancy of light speed $c_0 = \sqrt{as/2}$ to the natural consequence of the local homogeneity and intrinsic dynamics of the photino field, thereby breaking its necessary connection with space-time geometry.
3. **Reconstruction of Key Optical Phenomena:** Self-consistently deriving the hydrogen atomic spectrum, providing a unified explanation for various redshift phenomena, and accurately describing the gravitational deflection of light, all based on the photino field density distribution.

Thus, Photino Hypotheses I and II together constitute a coherent medium-dynamics paradigm, offering physical explanations for gravity and electromagnetic force, respectively, rooted in the microstructure of space-time. The following sections will systematically elaborate on the mathematical framework and empirical foundation of Photino Hypothesis II.

2 Field-Theoretic Reconstruction of the Nature of Light

To elucidate the nature of light within the unified framework of the Photino Hypothesis, it is first necessary to establish the microscopic foundation for the generation of electromagnetic waves. This chapter aims to reconstruct the binding mechanism of electrons within atoms and the excitation process of electromagnetic waves, starting from the dynamics of the photino field. It provides a complete theoretical description for the picture of the photon as a quantized field excitation.

2.1 Formation Mechanism of Atomic Electron Equilibrium Orbits

To establish the photino field excitation theory for electromagnetic waves, it is first essential to clarify the mechanism for the stable binding of electrons within atomic systems. Based on the

space-time medium framework established by Photino Hypothesis I [1], this section analyzes the origin of the quantized confinement of atomic electron orbits from a microscopic perspective, providing the theoretical foundation for the subsequent electromagnetic wave generation mechanism.

2.1.1 Electrostatic Balance Equation and Charge Distribution

Within the framework of photino theory, the stability of the nucleus-electron system is achieved through a dynamic balance between the nuclear Coulomb attraction and the repulsive force of the photino field. This balancing mechanism satisfies the following equation:

$$\frac{Ze^2}{4\pi\varepsilon_0 R_0^2} = \frac{dQ_p(r)\cdot e}{4\pi\varepsilon_0 r_{electron}^2} \qquad (2.1)$$

where:

- Z: Atomic nucleus charge number
- e: Elementary charge
- R_0: Ground state orbital radius of the hydrogen atom (Bohr radius)
- $dQ_p(r)$: Equivalent charge element of the photino acting on the electron
- $r_{electron}$: Effective distance from the photino element to the electron

The effective photino charge distribution acting on the electron is determined jointly by the electron's cross-sectional area and the photino field density gradient:

$$dQ_p(r) = \sigma_{pe}(r) \cdot A_e$$

where:

- $A_e = \pi r_e^2$ is the electron's cross-sectional area (r_e is the electron radius)
- $\sigma_{pe}(r) \propto r^{-2}$ characterizes the radial density distribution of the photino field

2.1.2 Orbital Stability Condition and Quantized Confinement

- **Nuclear Field Attraction:** Provides the centripetal force $F_c \propto r^{-2}$, pulling the electron towards the nucleus.
- **Photino Field Repulsion:** Establishes an inverse-square potential barrier $V(r) \propto r^{-2}$. When the electron moves towards the nucleus (decreasing r), the local photino density $\sigma_{pe}(r)$ increases sharply, generating a powerful radial repulsive force $F_r(r)$.

These two forces reach a dynamic equilibrium at a specific radius R_0, confining the electron to motion with uncertainty near the spherical surface defined by R_0. **This mechanism simultaneously explains the microscopic origin of why the electron does not collapse into the nucleus (due to the repulsive potential barrier) and its positional uncertainty (fluctuations under dynamic equilibrium).**

Summary: This section, based on the interaction between the photino field and the nuclear charge,

derives the stability condition for electron orbits within atoms. This model transforms the classical concept of an orbit into a probability distribution surface under dynamic equilibrium, laying the necessary field-theoretic foundation for discussing how the breaking of this balance (electron vibration) excites electromagnetic waves (photons) in the next section.

2.2 Mechanism of Electromagnetic Wave Generation and Photon Characteristics

Traditional electromagnetic theory describes the propagation of electromagnetic waves but does not reveal their microscopic generation mechanism. Quantum electrodynamics treats the photon as a point particle, failing to elucidate the origin of wave-particle duality. This section, based on the theory of atomic electron equilibrium orbits established in Section 2.1, proposes a photino field excitation mechanism. It interprets the photon as a quantized wave packet excited in the space-time medium by electron vibrations, providing a unified field-theoretic explanation for wave-particle duality.

2.2.1 Physical Mechanism of Electromagnetic Wave Excitation

Dynamics of Vibration Phase:

When an electron vibrates near its ground-state orbit R_0 and moves towards the high-density photino region $(r < R_0)$, the radial repulsive force it experiences is given by Eq. (2.1):

$$\boldsymbol{F_r(r) = \frac{\sigma_{pe}(r) A_e e}{4\pi\varepsilon_0 r_{electron}^2}} \qquad (2.2)$$

Energy Conversion and Conservation Mechanism:

The electron's kinetic energy E_k is converted into photino potential energy, satisfying the energy conservation relation:

$$\boldsymbol{E_k \rightarrow V(r) = -\int_{r_2}^{r_1} F_r(r) dr}$$

Potential Barrier Rebound and Periodic Vibration:

When the electron's kinetic energy $E_k < V(r)$, the repulsive potential barrier $V(r)$ causes the electron to rebound to the region outside the ground state $(r > R_0)$, forming a stable periodic vibration system. The vibration period is determined by the quantization condition:

$$\boldsymbol{T = \frac{2\pi}{\omega}, E = \hbar\omega}$$

2.2.2 Step-by-Step Analysis of the Dynamical Process

Photino Field Perturbation and Electromagnetic Wave Excitation (as shown in Fig. 2.1):

- The electron moves from the low-density region $(r > R_0)$ to the high-density region$(r \leq R_0)$, perturbing the photino field via the Coulomb force and exciting a transverse electromagnetic wave.
- **Exclusion Condition in Strong Gravitational Fields:** Within the Schwarzschild radius, photinos are bound by extreme gravity and cannot move freely, preventing the generation and transmission of electromagnetic waves [1].

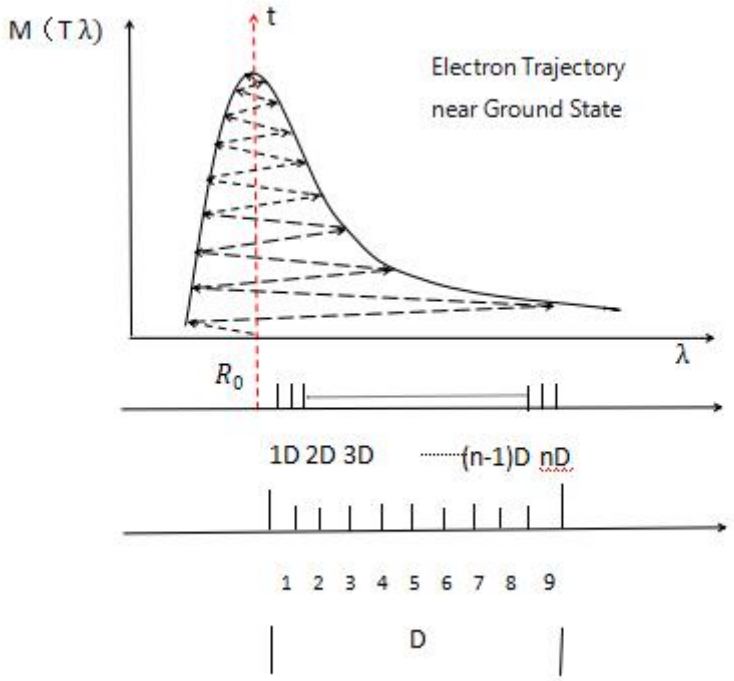

Fig. 2.1

Cascaded Excitation and Dynamics of the Vacuum Region:

- Each time the electron moves a characteristic distance $D_e = 2r_e$, it excites one train of electromagnetic waves, creating a photino vacuum region.
- The negative pressure in the vacuum region induces a circumferential backflow of photinos from adjacent areas. The backflow acceleration satisfies the dynamical relationship established in Photino Hypothesis I [1]:

$$\boldsymbol{a = \frac{nk_e q_p^2}{m_p r_p^2} \propto \frac{\sigma_{pe}(r)}{r_p^2} \propto \frac{Ze}{r^2}}$$

where r_p is the photino spacing and Z is the nuclear charge number. The backflow acceleration a determines the secondary wave excitation rate and frequency.

Wave Train Cascade and Frequency Generation:

- **Primary Wave Generation:** A circumferential primary wave is excited transversely and propagates at the speed of light.
- **Secondary Wave Cascade**: The primary wave returns to the center due to the negative pressure, colliding and exciting secondary waves, forming a chain reaction.
- **Frequency Determination Condition** (as shown in Fig. 2.2):

$$\boldsymbol{\nu \propto \frac{1}{\lambda} \propto a \propto \sigma_{pe}(r) \propto \frac{Ze}{r^2}} \qquad \textbf{(2.3)}$$

This relationship indicates: high-density photino field regions generate high-frequency photons; low-density regions correspond to low-frequency photons; the continuous variation in frequency

reflects the gradient distribution of the field density.

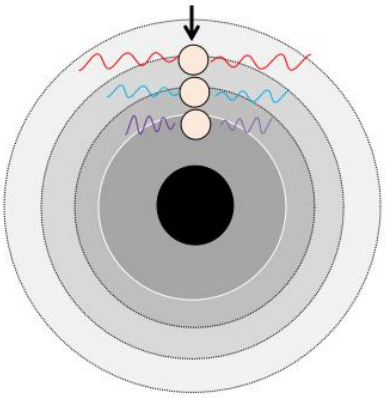

Fig. 2.2

2.2.3 Wave Packet Structure and Quantization Formation

Unique Amplitude and Wave Packet Attenuation:

- **Unique Amplitude**: Determined by the electron diameter, $A = D_e$.
- **Wave Packet Attenuation Mechanism**(as shown in Fig. 2.3):
  - Volume Attenuation: Volume of the n-th wave train $V_n = V_0/2^n$
  - Mass Dissipation: Mass of the n-th wave train $m_n = m_0(1-\alpha)^n$

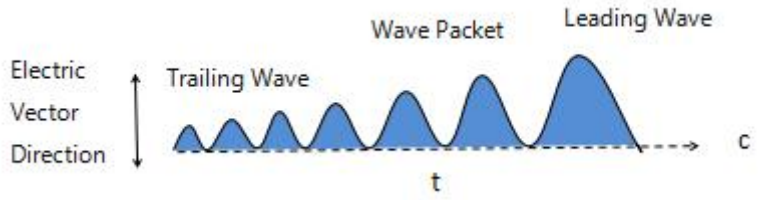

Fig. 2.3

Photon Quantization Interference Mechanism:

Electromagnetic waves of the same frequency superpose, forming quantized photons through constructive interference:

$$\boldsymbol{E_\gamma = h\nu}$$

Energy Conservation Relation:

$$\boldsymbol{\Delta E_k = \frac{1}{2}m_e v'^2 - \frac{1}{2}m_e v^2 = h\nu} \qquad (2.4)$$

Summary:

This electromagnetic wave excitation mechanism reveals, for the first time from a field-theoretic perspective, the microscopic origin of the photon. It directly links the mechanical vibration of the electron to the wave excitation of the photino field, providing a physical ontological explanation for wave-particle duality.

2.3 Theoretical Framework of the Speed of Light

Einstein elevated the constancy of the speed of light to a fundamental principle without revealing its underlying physical mechanism. Photino theory provides, for the first time, a dynamical foundation for this principle: the constancy of light speed originates from the intrinsic homogeneity of the space-time medium (the photino field) and the localized nature of its interactions.

2.3.1 Dynamical Interpretation of the Principle of Light Speed Constancy

Based on the photino field as the quantized carrier of the space-time background, its macroscopic propagation speed is jointly determined by the equivalent acceleration of momentum transfer between photinos and the characteristic displacement.

Dynamical Mechanism:

Light waves originate from the wave transfer generated by the excitation of the photino field due to electron displacement. This process achieves momentum exchange through the Coulomb repulsion between photinos. Considering the net force $F_i$on the i-th photino and its displacement S_i from rest to velocity v_i , the system satisfies the work-energy principle:

$$\boldsymbol{W = F_1 S_1 = F_2 S_2 = \cdots = F_n S_n}$$

where the net force on each photino is:

$$\boldsymbol{F_i = \frac{k_e q_p^2}{(r_p - S_{i-1})^2} - \frac{k_e q_p^2}{r_p^2}} \qquad \textbf{(2.5)}$$

Parameter Definitions:

- q_p: Photino equivalent charge
- r_p: Photino equilibrium spacing
- $k_e = 1/(4\pi\varepsilon_0)$: Coulomb constant
- S_{i-1}: Displacement of the preceding photino

Proof of Displacement Consistency:

Under the small displacement approximation $(S_i \ll r_p)$, perform a Taylor expansion of the net force:

$$\boldsymbol{F_i = \frac{k_e q_p^2}{r_p^2}\left(\frac{2S_{i-1}}{r_p} + \frac{3S_{i-1}^2}{r_p^2} + O(S_{i-1}^3)\right)}$$

Taking the first-order approximation $F_i \approx \frac{2k_e q_p^2}{r_p^3} S_{i-1}$and substituting into the work-energy principle:

$$\boldsymbol{F_1S_1 = F_2S_2 \Rightarrow S_0S_1 = S_1S_2 \Rightarrow S_0 = S_2}$$

$$\boldsymbol{F_2S_2 = F_3S_3 \Rightarrow S_1S_2 = S_2S_3 \Rightarrow S_1 = S_3}$$

By induction, all displacements are consistent:

$$\boldsymbol{S_0 = S_1 = S_2 = \cdots = S_n = S} \qquad \textbf{(2.6)}$$

Microscopic Derivation of the Intrinsic Light Speed:

The constancy of the local photino spacing r_p and the displacement consistency lead to a constant net force F, and consequently a constant acceleration a:

$$\boldsymbol{a = \frac{F}{m_p} =}\textbf{constant}$$

The macroscopic propagation speed of a photon is defined as the ratio of the characteristic displacement S to the characteristic time τ required to complete that displacement:

$$\boldsymbol{c_0 = \frac{S}{\tau}}$$

From the kinematic formula $S = \frac{1}{2}a\tau^2$, solve for the characteristic time $\tau = \sqrt{2S/a}$, and substitute into the above equation:

$$\boldsymbol{c_0 = \frac{S}{\sqrt{\frac{2S}{a}}} = \sqrt{\frac{aS}{2}}} \qquad \textbf{(2.7)}$$

Connection to Classical Electromagnetic Theory:

Relate to the light speed expression derived from Maxwell's equations:

$$\boldsymbol{c_0 = \frac{1}{\sqrt{\varepsilon_0\mu_0}} = \sqrt{\frac{aS}{2}}}$$

That is:

$$\boldsymbol{aS = \frac{2}{\varepsilon_0\mu_0}} \qquad \textbf{(2.8)}$$

This equation indicates that the vacuum permittivity ε_0 and vacuum permeability μ_0 are not fundamental constants; rather, they reflect the intrinsic dynamical property of the space-time photino field—the product of acceleration a and characteristic displacement S.

Experimental Verification:

- **Michelson-Morley Experiment:** The Earth's positive electric field exerts a "**locking effect**" on photinos (Coulomb locking force $F_{\text{Coulomb}} = k_e\left(MQ_{m0}q_p\right)/r^2$). This force binds photinos to

be stationary relative to the Earth's surface, eliminating the drift expected by the aether hypothesis and ensuring the measured light speed is isotropic:

$$\boldsymbol{\Delta c = 0 \Longrightarrow c_{\text{measured}} = c_0}$$

- **GPS Satellite Clock Corrections**: Relativistic corrections rely on the invariance of c_0. The locally measured light speed is consistently $299{,}792{,}458\text{m/s}$, verifying the c_0 invariance maintained by the locking effect.

This theoretical framework for light speed reveals the physical origin of light speed constancy from a microscopic dynamical perspective, providing solid field-theoretic support for the foundation of relativity.

2.3.2 The Nature and Correction of Apparent Light Speed Variability

Phenomenological Mechanism of Apparent Light Speed Variability:

The observed phenomena of light speed variation under specific conditions are essentially apparent effects caused by the overall motion of the photino field or changes in the propagation path, not a real alteration of the intrinsic light speed value c_0.

Apparent Light Speed Change due to Field Motion:

When the photino field moves as a whole relative to the observer's frame, as observed in phenomena like the Fizeau water flow experiment, the apparent light speed obeys the velocity addition formula:

$$\boldsymbol{c = \frac{c_0}{n} \pm v\left(1 - \frac{1}{n^2}\right)} \qquad \textbf{(2.9)}$$

where:

- v: Overall velocity of the photino field
- n: Refractive index of the medium, characterizing its ability to bind photinos
- The second term $\pm v(1 - 1/n^2)$ reflects the Fresnel drag effect, with the sign depending on the relationship between the field's motion direction and the photon's propagation direction.

The Nature of "Light Speed Reduction" in Media:

When photons pass through a medium, energy exchange with the medium's extranuclear electrons induces disturbances such as lattice vibrations and thermal fluctuations. This causes oscillations in the local photino field and produces a drag effect, resulting in a lower apparent light speed:

$$\boldsymbol{\mathrm{c}_{\text{apparent}} = \frac{s_{\text{apparent}}}{t_{\text{text\{actual}}} < c_0(\text{not a real reduction})}$$

Core Mechanism Analysis:

- **Path Elongation**: The actual propagation path of the photon in the medium $s_{actual} > s_{apparent}$, where $s_{apparent}$ is the geometric thickness of the medium.
- **Time Delay:** The interaction between the photon and atoms leads to an effective propagation time $t_{actual} > t_{free} = s_{apparent}/c_0$.
- **Invariance of Intrinsic Speed:**
  - **Confirmed by single-photon experiments:** The speed during free propagation segments before the photon enters and after it leaves the medium is strictly c_0 [2].
  - **Indicated by ultrafast laser measurements**: The instantaneous speed of photons not absorbed within the medium remains c_0 [3,4]. The apparent "reduction" stems solely from energy residence time.

Theoretical Advantages of the Photino Model:

1. **Unified Explanation of Apparent Phenomena:** Path elongation ($s_{actual} > s_{apparent}$) + time delay ($t_{actual} > t_{free}$)⟶ apparent reduction.
2. **Compatibility with Quantum Effects**: Single-photon experiments confirm constant speed c_0 in free segments (no need to introduce specific assumptions like "photon rest mass") [2]; quantum entanglement information is transmitted at c_0 (unaffected by media) [5].
3. **Resolution of Theoretical Contradictions:** The instantaneous change in light speed at medium boundaries is naturally explained; the universality of the relativistic principle of light speed constancy is preserved.

This correction theory clarifies that the nature of apparent light speed variability is an effect due to changes in propagation conditions, providing a unified field-theoretic framework for understanding light propagation behavior in complex media.

2.4 Photon Energy – Kinetic Mass Relationship

Based on the photino field excitation theory, this section systematically elaborates on the intrinsic connection between photon energy and kinetic mass, derives the microscopic origin of photon kinetic mass from a field-theoretic perspective, and establishes its quantitative relationship with photino field density.

2.4.1 Field-Theoretic Derivation of Photon Kinetic Mass

Momentum Definition and Energy Expression

Within the framework of photino theory, the momentum of a photon is defined as:

$$p = m_\gamma c_0$$

Photon energy originates from the collective kinetic energy of excited photinos. Considering the total work done in accelerating N photinos to a final velocity v':

$$\boldsymbol{E_\gamma = \int_0^S F \cdot dr = N\left[\int m_p \frac{dv}{dt} \cdot v dt\right] = N\left[m_p \int_0^{v'} v dv\right] = \frac{1}{2} N m_p (v')^2}$$

Kinematic Relation and Equivalent Mass Definition

Substituting the kinematic relation $v' = \sqrt{2aS}$ and the relation $aS = 2c_0^2$ derived from the principle of light speed constancy:

$$\boldsymbol{E_\gamma = \frac{1}{2} N m_p (2aS) = N m_p aS = N m_p (2c_0^2) = 2N m_p c_0^2}$$

Within this theoretical framework, the kinetic mass of the photon is defined as the equivalent mass corresponding to its energy:

$$\boldsymbol{m_\gamma = \frac{E_\gamma}{c_0^2} = 2N m_p} \qquad \textbf{(2.10)}$$

Here, N is the effective excitation number characterizing the energy transfer efficiency of the photino field. **Physically, $2Nm_p$ corresponds to the total inertial mass of all excited photinos required to constitute a complete photon (comprising one wave crest and one trough)**.

Field-Theoretic Basis of the Energy-Frequency Relationship

Combining with the fundamental quantum mechanical relation $E_\gamma = h\nu_0$, we obtain:

$$\boldsymbol{E_\gamma = m_\gamma c_0^2 = h\nu_0} \qquad \textbf{(2.11)}$$

This derivation naturally leads, from a field-theoretic level, to the following:

1. **Quantization of Photon Energy**: $E_\gamma = h\nu_0$ stems from the discrete excitation characteristics of the photino field.
2. **Essence of Zero Rest Mass**: The zero rest mass of the photon, $m_0 = 0$, is naturally derived from the condition that its energy originates entirely from kinetic mass, without the need for ad hoc assumptions.
3. **Physical Meaning of Kinetic Mass:** $m_\gamma = h\nu_0 / c_0^2$ characterizes the inertial response of the photon during field propagation.

Correspondence with Classical Theory

When the photino field approaches the continuous limit, this theory reduces to classical electromagnetic theory:

- **Wave Energy Density**: Consistent with the energy density expression of classical electromagnetic waves.

- **Momentum Transfer**: Compatible with the classical description of radiation pressure.
- **Quantization Transition:** In the macroscopic limit, discrete quantization tends towards a continuous energy spectrum.

This derivation provides a solid field-theoretic foundation for understanding the particle nature of photons, unifying the wave nature of electromagnetic waves and the particle nature of photons at the level of microscopic mechanisms.

2.4.2 Density Dependence of Intrinsic Frequency and Kinetic Mass

Based on the field-theoretic framework for photon kinetic mass established above, this section explores the dependence of the photon's intrinsic frequency and kinetic mass on the density of the photino field, revealing the microscopic origin of quantized energy levels.

Direct Relationship Between Kinetic Mass and Field Density

Combining the energy-frequency relation $E_\gamma = h\nu_0 = m_\gamma c_0^2$ with the frequency-density relation (2.3), we obtain:

$$\boldsymbol{m_\gamma = \frac{h\nu_0}{c_0^2} \propto \nu_0 \propto \sigma_{pe}(r)} \qquad \textbf{(2.12)}$$

Interpretation of Physical Significance:

1. **Origin of Mass:** The kinetic mass of the photon originates from the collective inertia of the excited photinos.
2. **Density Modulation:** The density gradient of the photino field naturally modulates the photon's energy and mass.
3. **Foundation of Quantization:** The discrete distribution of field density provides the physical basis for energy level quantization.

This density dependence reveals the continuous field-theoretic essence behind apparent quantization phenomena. As an excitation of the photino field, all apparent quantum properties of the photon — energy, frequency, momentum — are continuously determined by the density distribution of the space-time medium.

Summary

This chapter establishes the photino field excitation theory for electromagnetic waves and photons. The core breakthroughs include:

1. **Reconstruction of Photon Essence:** Interpreting the photon as a quantized excitation of the photino field, unifying the physical essence of wave-particle duality.
2. **New Interpretation of Light Speed Constancy**: Deriving $c_0 = \sqrt{aS/2}$ from medium dynamics, providing a new interpretation for the foundation of relativity.
3. **Basis for Spectral Phenomena**: Establishing the relationship between photon properties and

field density, $\nu_0, m_\gamma \propto \sigma_{pe}(r)$, providing a continuous field-theoretic explanation for quantum phenomena.

This theory reduces the concept of "transition" in quantum mechanics to a process of continuous field interaction, providing a unified microscopic basis for understanding various phenomena from atomic spectra to cosmological redshift. This theoretical framework represents a fundamental shift from the traditional quantum paradigm to a medium-dynamics paradigm. Subsequent chapters will systematically derive and verify specific physical phenomena based on this foundation.

3 Field-Theoretic Explanation of Key Optical Phenomena

This chapter will provide a unified field-theoretic explanation for several key optical phenomena, based on the photino field excitation theory established in Chapter 2. By reducing apparent quantization phenomena to processes of continuous field interaction, the theory demonstrates its self-consistency and explanatory power in describing physical phenomena from the atomic to the cosmic scale.

3.1 Field-Theoretic Derivation of the Hydrogen Atomic Spectrum

The hydrogen atomic spectrum is one of the most classic verifications of quantum theory. This section aims to re-derive the hydrogen spectral series based on the density distribution of the photino field, reducing the Bohr model picture of energy level transitions to the natural outcome of the continuous motion of an electron within the photino field.

3.1.1 Physical Background and Core Assumptions

Hydrogen, as the most abundant element in the universe (approximately 75%), serves as a crucial probe in stellar physics and cosmology. Based on the Photino Hypothesis, the formation mechanism of the hydrogen atomic spectrum rests on the following core physical picture and assumptions (as shown in Fig. 2.1):

1. **Ground State Orbital Constraint**: The electron is dynamically confined near the spherical surface defined by the ground-state radius R_0 (Bohr radius). Its stability is ensured by the balance between the nuclear Coulomb attraction and the radial repulsive force of the photino field (see Section 2.1).
2. **Field Density Distribution Law:** The effective surface density of the photino field follows a strict inverse-square distribution [1]:

$$\boldsymbol{\sigma_{pe}(r) = R_e \frac{e}{r^2}}$$

where $R_e$is a parameter related to space-time geometry. This distribution forms the field-theoretic basis for the discreteness of spectral lines.

3. **Quantized Displacement Condition**: The stimulated "transition" of the electron manifests as a

quantized radial displacement. Each movement by one electron characteristic diameter $D_e = 2r_e$ excites a train of electromagnetic waves with a specific frequency.

3.1.2 Energy Level Transitions and Electromagnetic Wave Excitation

Quantized Displacement Path: The stimulated electron undergoes quantized displacement from the ground state R_0 towards the atomic nucleus:

$$\boldsymbol{r_n = R_0 + nD_e(n = 1,2,3,\ldots)}$$

Single Wave Train Energy Mechanism: The energy of each electromagnetic wave train is determined by the photino field density gradient along the displacement path. Combining Eq. (2.11) and Eq. (2.3) yields:

$$\boldsymbol{E_\gamma = h\nu = m_\gamma c_0^2 \propto \sigma_{pe}(r) \propto \frac{1}{r^2}}$$

Multiple Wave Train Generation: When the electron moves a distance of $n \cdot D_e$, it excites n trains of electromagnetic waves sequentially. The frequency of the k-th wave train is determined by the photino density $\sigma_{pe}(r_k)$ in that displacement segment.

Cascade Transitions and Frequency: When the electron relaxes from a higher energy level r_{n+1} to a lower level r_n, the frequency of the emitted photon is governed by the difference in photino density between the start and end points:

$$\boldsymbol{\nu_{n\to m} \propto \sigma_{pe}(r_n) - \sigma_{pe}(r_m)(m\rangle n)}$$

Rebound Cutoff and Metastable State Cycle (as shown in Fig. 2.1):

- **Role of the Repulsive Potential Barrier:** When the electron enters the high-density photino region near the nucleus$(r < R_0)$, it encounters a sharply increasing repulsive force, causing a rebound and terminating the generation of the current wave train.
- **Elastic Rebound Path**: After losing energy $\Delta E = \sum h\nu$, the electron rebounds to a series of metastable energy levels $(n-\delta)D_e$ (where $0<\delta<1$), forming a chain relaxation cycle: $(n-\delta) \to (n-2\delta) \to \ldots \to R_0$. This process is the physical basis for generating the fine structure of spectral lines.

3.1.3 Energy Distribution and Matching with Blackbody Radiation

Ground State Crossing Dominance Mechanism: In the chain relaxation process, the frequency of the electron crossing the vicinity of the ground state $R_0$is highest (see Fig. 2.1). The corresponding energy accumulation forms the peak region of the radiation energy spectrum.

Frequency-Energy Distribution Characteristics:

- **High-Frequency Region** $(r < R_0)$: The photino density is high, leading to high-energy excited photons. However, the probability of an electron traversing this region is relatively low, so energy increases steeply with frequency.

- **Low-Frequency Region** $(r > R_0)$: The photino density is low, leading to low-energy excited photons. However, the probability of the electron being in this outer region is high, and the path length is significant, so energy decreases smoothly with frequency.

Natural Derivation of the Blackbody Radiation Spectrum: The energy distribution determined by the continuous density gradient of the photino field statistically and naturally leads to the form of the Planck blackbody radiation spectrum, without the need for ad hoc assumptions such as quantum harmonic oscillators:

$$\boldsymbol{B_\nu(T) = \frac{2h\nu^3}{c^2}\frac{1}{e^{h\nu/k_BT} - 1}}$$

Here, within this framework, the temperature T is associated with the statistical distribution of the electron's average kinetic energy within the photino field. This provides a microscopic field-theoretic foundation for understanding thermal radiation phenomena.

3.1.4 Derivation of the Hydrogen Atomic Spectral Line Equation

This section derives the precise mathematical form of the hydrogen spectral line equation based on the principle of energy conservation. The process of the electron overcoming the field force within the photino field is quantified as photon energy, naturally leading to a wavelength expression consistent with the Rydberg formula.

1. Energy Conservation and Photon Energy Conversion

Based on energy conservation, when an electron transitions from energy level r_m to level $r_n(m\rangle n$, displacement of $(m-n)$ electron diameters), the work done against the radial repulsive force of the photino field $F_r(r)$ is completely converted into the energy of one photon, $h\nu$. For a single wave train generated by a unit displacement (one electron diameter D_e, its energy expression is:

$$\boldsymbol{h\nu_{n+1\to n} = \int_{r_{n+1}}^{r_n} F_r\,(r)dr = \int_{r_{n+1}}^{r_n} \frac{k_e e dQ_p(r)}{r^2}} \qquad \textbf{(3.1)}$$

where:

- $dQ_p(r) = \sigma_{pe}(r)A_e$ is the equivalent charge element of the photino acting on the electron.
- The integration path corresponds to the electron position changing from r_{n+1} to r_n, or equivalently, the charge changing from $Q_p(r_{n+1})$ to $Q_p(r_n)$.

2. Integral Variable Transformation and Analytical Solution

Since the electron moves a fixed distance D_e, and the change in the photino charge element is approximately linearly related to the displacement ($dQ_p/dr \approx$ constant), while the denominator r^2 can be characterized by the characteristic scale D_e under local approximation, Eq. (3.1) can be simplified to:

$$h\nu_{n+1\to n} = \int_0^{D_e} \frac{k_e e dQ_p(r)}{r^2} dr \approx \int_{Q_p(r_n)}^{Q_p(r_{n+1})} \frac{k_e e}{D_e} dQ_p(r)$$

Performing the integration yields:

$$h\nu_{n+1\to n} = \frac{k_e e}{D_e}\left[Q_p(r_n) - Q_p(r_{n+1})\right] \qquad (3.2)$$

3. Equivalent Charge Expression and Frequency Equation

Substituting the expression for the equivalent photino charge, $Q_p(r) = \sigma_{pe}(r)A_e = (R_e e/r^2) \cdot \pi(D_e/2)^2$, into Eq. (3.2):

$$h\nu_{n+1\to n} = \frac{k_e e}{D_e}\left[\frac{R_e e\pi D_e^2}{4r_n^2} - \frac{R_e e\pi D_e^2}{4r_{n+1}^2}\right] = \frac{R_e k_e e^2 \pi D_e}{4}\left(\frac{1}{r_n^2} - \frac{1}{r_{n+1}^2}\right) \qquad (3.3)$$

4. Quantization Condition and Wavelength Equation

Introducing the quantization condition: $r_n = nD_e, r_{n+1} = (n+1)D_e$. Substituting into Eq. (3.3) and rearranging gives:

$$\nu_{n+1\to n} = \frac{R_e k_e e^2 \pi}{4hD_e}\left(\frac{1}{n^2} - \frac{1}{(n+1)^2}\right) \qquad (3.4)$$

To correspond with the experimentally observed wavelength form, we transform using $\nu = c_0/\lambda$ and the Coulomb constant $k_e = 1/(4\pi\varepsilon_0)$:

$$\frac{1}{\lambda_{n+1\to n}} = \frac{R_e k_e e^2 \pi}{4hc_0 D_e}\left(\frac{1}{n^2} - \frac{1}{(n+1)^2}\right) = \frac{R_e e^2}{16\varepsilon_0 hc_0 D_e}\left(\frac{1}{n^2} - \frac{1}{(n+1)^2}\right)$$

Introducing the reduced Planck constant $\hbar = h/(2\pi)$ yields a more compact form:

$$\frac{1}{\lambda_{n+1\to n}} = \frac{R_e}{8D_e} \cdot \frac{e^2}{4\pi\varepsilon_0 \hbar c_0}\left(\frac{1}{n^2} - \frac{1}{(n+1)^2}\right) \qquad (3.5)$$

5. Explicit Inclusion of the Fine Structure Constant

Defining the fine structure constant α as:

$$\alpha = \frac{e^2}{4\pi\varepsilon_0 \hbar c_0} \approx \frac{1}{137}$$

The hydrogen atomic spectral line equation can finally be expressed concisely as:

$$\frac{1}{\lambda_{n+1\to n}} = \frac{R_e \alpha}{8D_e}\left(\frac{1}{n^2} - \frac{1}{(n+1)^2}\right) \qquad (3.6)$$

This equation is mathematically identical in form to the empirical Rydberg formula, where the proportionality coefficient $\frac{R_e\alpha}{8D_e}$corresponds to the Rydberg constant R_H. This derivation naturally

yields the quantized characteristics of the hydrogen atomic spectrum from the continuous dynamical process of photino field interaction, indicating that the apparent energy level transition is essentially the natural result of electron motion under the density gradient of the photino field.

3.1.5 Theoretical Verification and Experimental Consistency

This section aims to systematically compare the hydrogen atomic spectral line equation derived from the photino field theory with high-precision experimental observations, verifying the self-consistency of its mathematical form and physical parameters, and expounding its explanatory power and theoretical predictions for spectral fine structures.

1. Formal Consistency with the Rydberg Formula

The spectral line equation derived from the photino model (Eq. 3.6) is completely consistent in mathematical form with the empirical Rydberg formula.

Theoretically Derived Formula:

$$\frac{1}{\lambda} = \frac{R_e \alpha}{8 N D_e}\left(\frac{1}{n^2} - \frac{1}{m^2}\right) \ (m > n)$$

Empirical Rydberg Formula:

$$\frac{1}{\lambda} = R_H\left(\frac{1}{n^2} - \frac{1}{m^2}\right)$$

Coefficient Equivalence Relation:

Comparing the coefficients yields the relationship between the photino theory parameters and the Rydberg constant R_H:

$$R_e = \frac{8 D_e R_H}{\alpha} \qquad (3.7)$$

This relation is the key bridge connecting microscopic space-time geometry parameters (R_e, D_e) with macroscopic observational constants (R_H, α).

2. Self-Consistent Calculation of Microscopic Space-Time Geometry Parameters

Substituting known physical constants into Eq. (3.7) allows solving for the theoretically predicted microscopic parameter R_e.

- **Values of Experimental Constants:**
  - Rydberg constant $R_H = 1.097373 \times 10^7 \mathrm{m}^{-1}$
  - Fine-structure constant $\alpha \approx 1/137.036$
  - Classical electron diameter $D_e = 2r_e$. The current upper limit for the electron radius from particle physics experiments is $r_e < 10^{-22}\mathrm{m}$ (90% confidence level) [6]. For parameter estimation, taking its critical value $r_e = 1.0 \times 10^{-22}\mathrm{m}$, then $D_e \approx 2.0 \times 10^{-22}\mathrm{m}$.

Calculation:

$$R_e = \frac{8 \times (2.0 \times 10^{-22}\mathrm{m}) \times (1.097 \times 10^{7}\mathrm{m}^{-1})}{1/137.036} \approx 2.40 \times 10^{-12}(\text{dimensionless})$$

The obtained R_e is a dimensionless space-time geometry parameter. Its order of magnitude is consistent with expectations, verifying the self-consistency of the theoretical parameter system.

3. The Intrinsic Nature of the Fine-Structure Constant

The theory naturally introduces the fine-structure constant in its derivation:

$$\boldsymbol{\alpha = \frac{e^2}{4\pi\varepsilon_0 \hbar c_0}}$$

Deepened Physical Significance:

- **Electromagnetic Coupling Strength**: In photino theory, α characterizes the inherent strength of the interaction between the electron and the photino field.
- **Field-Theoretic Foundation**: As a dimensionless constant, the emergence of α indicates that the strength of the electromagnetic interaction is rooted in the intrinsic properties of the space-time medium (the photino field), not an extrinsic parameter.
- **Connection to QED:** This constant is numerically and physically identical to the fine-structure constant in Quantum Electrodynamics (QED). This indicates that photino field theory is an underlying field-theoretic description of the electromagnetic interaction, compatible with the existing most precise quantum theoretical framework.

4. Theoretical Explanation of Spectral Fine Structure

Based on the photino field density distribution $\sigma_{pe}(r) \propto r^{-2}$ and the details of its dynamics, the theory can naturally explain fine phenomena in the hydrogen atomic spectrum:

- **Energy Level Splitting**: There are subtle differences in the effective photino field distribution traversed by electron orbits with different angular momenta (s, p, d⋯). This leads to slightly different equivalent potential energies for the same principal quantum number n, naturally forming fine splitting of energy levels.
- **Lamb Shift**: Traditionally attributed in QED to quantum fluctuations of the vacuum electromagnetic field [7, 8]. In photino theory, this is reconstructed as a perturbation to the electron's equilibrium position within the atom due to "**dynamic fluctuations of the photino field density**". Fluctuations arising from the intrinsic dynamics of the photino field itself can similarly produce small energy shifts in the levels.
- **Hyperfine Structure**: Originates from inelastic rebound processes caused by photino Coulomb repulsion. During the relaxation process, part of the electron's energy is converted into exciting secondary wave trains or induces slight changes in nuclear spin orientation, resulting in finer level splitting.

5. Universal Verification with Multi-Element Spectra

The theoretical framework can be naturally extended to multi-electron atomic systems. In this case, the effective photino field density acting on an outer electron must account for the shielding effect of inner electrons, corrected to:

$$\boldsymbol{\sigma_{pe}(r) = R_e \frac{Z_{eff} e}{r^2}}$$

where Z_{eff} is the effective nuclear charge number $\left(Z_{eff} < Z\right)$. This corrected model can explain:

- **Alkali Metal Spectra**: The valence electron moves within the combined shielded Coulomb field and photino field created by the nucleus and inner electrons. Their spectral series are similar to hydrogen's but exhibit shifts.
- **X-ray Characteristic Spectra**: Inner electron transitions occur in regions of strong effective nuclear charge $\left(Z_{eff} \approx Z\right)$, producing high-frequency characteristic X-rays. Their energy is proportional to $(Z-1)^2$ (Moseley's law), consistent with the corrected relation $\sigma_{pe}(r) \propto Z_{eff}/r^2$.
- **Molecular Spectra**: The formation of chemical bonds alters the local charge distribution around atomic nuclei, thereby modulating the photino field density $\sigma_{pe}(r)$ in that region. This causes changes in vibrational-rotational energy levels of electrons, providing a microscopic mechanism at the field-theoretic level for molecular spectra.

Summary: This section systematically verifies the high consistency between the predictions of the photino field theory for the hydrogen atomic spectrum and experimental observations. The theory not only self-consistently derives the mathematical form of the Rydberg formula and imbues the fine-structure constant with new physical meaning, but also provides a unified explanatory framework based on field density modulation for spectral fine structures and multi-element spectral phenomena. This marks a fundamental shift from the traditional quantum mechanics paradigm of "energy level transitions" to a dynamics paradigm based on interactions within a continuous space-time medium (the photino field).

3.2 Unified Field-Theoretic Explanation of Redshift Mechanisms

This chapter aims to construct a unified framework based on photino field dynamics to explain gravitational redshift and cosmological redshift phenomena. The core idea is to attribute the essence of redshift to the modulation effect experienced by the photon kinetic mass as it propagates through a non-uniform photino field, thereby providing a coherent field-theoretic

description for redshift occurring at different scales and under various physical conditions.

3.2.1 Gravitational Redshift

1. The Physical Essence and Microscopic Mechanism of Redshift

Within the framework of photino theory, the physical essence of gravitational redshift and blueshift is that as a photon wave packet propagates through a gravitational potential gradient, the photinos within it experience dynamic drag (or repulsion). This leads to a change in the photon's equivalent kinetic mass m_γ, which in turn causes a change in frequency and wavelength.

Analysis of the Microscopic Mechanism:

The photino field density distribution $\sigma_{pm}(r)$ is modulated by the gravitational potential Φ_g near a massive celestial object. The photon carries an equivalent charge $Q_\gamma = m_\gamma Q_{p/m}$ (where $Q_{p/m}$ is the photon's charge-to-mass ratio), which experiences a force in this gradient field. The energy conservation relation determines how the frequency (or kinetic mass) changes with position.

- **Propagation along the gravitational direction** (e.g., towards the gravitational source): Gravity produces a forward drag on the photinos, causing them to converge into the wave packet. This results in $\Delta m_\gamma > 0$, increasing the photon energy and frequency, manifesting as a **blueshift** （$\lambda \downarrow$）.
- **Propagation against the gravitational direction** (e.g., escaping from a gravitational source): Gravity produces a reverse drag on the photinos, partially stripping them from the wave packet. This results in $\Delta m_\gamma < 0$, attenuating the photon energy and reducing its frequency, manifesting as a **redshift** （$\lambda \uparrow$）.

2. Field-Theoretic Derivation of the Gravitational Redshift Formula

Analysis of the Force on the Photon:

Consider a celestial object of mass M with a mass-equivalent charge Q_{m0}. At a distance \(r\) from the object's center, the force on the photon can be expressed as:

$$\boldsymbol{F = Q_\gamma E_M = \frac{k_e M Q_{m0} m_\gamma Q_{p/m}}{r^2}} \qquad \textbf{(3.8)}$$

where E_M is the equivalent field strength generated by the object.

Energy Conservation Equation:

Let the photon's kinetic mass be $m_\gamma$and its frequency be ν at position r. After propagating to position R(R > r), its kinetic mass becomes $m_\gamma{}'$ and its frequency becomes $m_\gamma{}'$. Considering the conservation of the sum of the photon's kinetic energy and its potential energy in the field:

$$\left(m_\gamma{}' c_0^2 - \frac{k_e M Q_{m0} m_\gamma{}' Q_{p/m}}{R}\right) = \left(m_\gamma c_0^2 - \frac{k_e M Q_{m0} m_\gamma Q_{p/m}}{r}\right)$$

Frequency (Kinetic Mass) Ratio Expression:

Rearranging the above equation yields the ratio of the photon's kinetic mass before and after escaping the gravitational field. Combining with the relation $m_\gamma \propto \nu$, we have:

$$\frac{\nu}{\nu'} = \frac{m_\gamma}{m_\gamma{}'} = \frac{1 - \frac{k_e M Q_{m0} Q_{p/m}}{c_0^2 R}}{1 - \frac{k_e M Q_{m0} Q_{p/m}}{c_0^2 r}} \qquad (3.9)$$

Redshift Expression:

According to the definition of redshift $z = \nu/\nu' - 1$, substituting Eq. (3.9) yields:

$$z = \frac{1 - \frac{k_e M Q_{m0} Q_{p/m}}{c_0^2 R}}{1 - \frac{k_e M Q_{m0} Q_{p/m}}{c_0^2 r}} - 1 \qquad (3.10)$$

Limiting Cases for Observation:

- Propagation from the stellar surface (r) to infinity $(R \to \infty)$:

  Let $u = \frac{k_e M Q_{m0} Q_{p/m}}{c_0^2 r}$, then the redshift simplifies to:

$$z = \frac{1}{1-u} - 1$$

- **Weak-field approximation** $(u \ll 1)$: Performing a Taylor expansion on the above expression gives:

$$z \approx u + u^2 + O(u^3) \approx \frac{k_e M Q_{m0} Q_{p/m}}{c_0^2 r} \qquad (3.11)$$

3. Parameter Self-Consistency and Correspondence with Classical Theory

To ensure compatibility of the theory with existing experimental verification, it is necessary to establish a connection between the photino parameters and the macroscopically observed gravitational constant G. Based on the microscopic expression for the gravitational constant established in Photino Hypothesis I, $G = R_m k_e Q_{m0}^2$ [1], and requiring that Eq. (3.11) in the weak-field limit agrees with the prediction of General Relativity $z \approx GM/(c_0^2 r)$, we obtain the following key relation:

$$G = k_e Q_{m0} Q_{p/m} \qquad (3.12)$$

Combining the known macroscopic space-time geometry parameter $R_m = 1.436 \times 10^{15}$ and the mass-equivalent charge $Q_{m0} = 2.276 \times 10^{-18}\mathrm{C/kg}$ [1], we can self-consistently derive the charge-to-mass ratio of the photon:

$$\boldsymbol{Q_{p/m} = \frac{G}{k_e Q_{m0}} \approx 3.3 \times 10^{-3}\mathrm{C/kg}}$$

This derivation not only verifies the intrinsic self-consistency of the theoretical system but, more importantly, establishes the identity between the photon's charge-to-mass ratio $Q_{p/m}$ and the intrinsic charge-to-mass ratio of the photino. This builds a solid bridge between microscopic field parameters and macroscopic gravitational phenomena.

4. Strong-Field Correction: Enhancement Effect of the Equivalent Gravitational Constant

In the strong gravitational field environments of compact objects (such as neutron stars, black holes), according to the mechanism proposed in Photino Hypothesis I, electrons outside the atomic nucleus may be compressed into the nucleus, leading to a weakening or disappearance of the electron shielding effect. This causes an increase in the equivalent charge Q_{m0} of the massive body [1]. Based on$G = R_m k_e Q_{m0}^2$, we introduce a correction factor β related to the compactness of the celestial object:

$$\boldsymbol{\beta \equiv 1 + f(M,\rho) \geq 1}$$

where $f(M,\rho)$ is a function of mass M and density ρ, characterizing the degree of electron collapse. The corrected effective gravitational constant is:

$$\boldsymbol{G' = R_m k_e (\beta Q_{m0})^2 = \beta^2 G}$$

Therefore, after considering the gravitational enhancement effect of compact matter, the redshift formula (3.11) under the weak-field approximation should be corrected to:

$$\boldsymbol{z \approx \frac{\beta^2 G M_{\mathrm{compact}}}{c_0^2 r}} \qquad \textbf{(3.13)}$$

For a system containing both compact matter M_{compact} and ordinary visible matter $M_{\mathrm{text\{visible}}$, the total redshift can be written as the superposition of their contributions:

$$\boldsymbol{z \approx \frac{G}{c_0^2 r}\left[\beta(r)^2 M_{\mathrm{compact}}(r) + M_{\mathrm{isible}}(r)\right]}$$

This correction mechanism provides a new theoretical framework for explaining the anomalously large gravitational redshifts observed for some compact celestial objects. This is a key testable prediction that distinguishes this theory from General Relativity.

3.2.2 Cosmological Redshift

Cosmological redshift is commonly interpreted as the stretching of light wavelengths due to the expansion of cosmic space. Within the framework of photino theory, we propose a novel physical mechanism—the "**photon fatigue effect**"—which attributes cosmological redshift to the intrinsic energy attenuation of photons due to prolonged interaction with the cosmic-scale photino

field. This provides a field-theoretic explanation for **Hubble's law** that is independent of spatial expansion.

1. Principle of the Fatigue Mechanism and Equation Derivation

Physical Picture:

As photons propagate across large-scale cosmic space, they continuously undergo weak inelastic interactions with the uniformly distributed photino field (primarily manifesting as mutual repulsive scattering among photinos). This interaction exerts a damping force on the photon that is proportional to its instantaneous energy, causing its energy to decay exponentially with propagation distance.

Damping Force Expression:

Let the damping force f exerted by the photino field on the photon be proportional to the photon's instantaneous energy E:

$$\boldsymbol{f = \alpha E = \alpha h \nu}$$

where α is the damping coefficient (dimensions m^{-1}), characterizing the intrinsic strength of the photino field in dissipating photon energy.

Energy Attenuation Differential Equation:

The work done by the photon to overcome this damping force leads to a reduction in its energy. Considering a differential propagation distance dD, the energy loss dE equals the work done against the damping force:

$$\boldsymbol{dE = -\, f \cdot dD = -\, \alpha E \cdot dD}$$

Solving the Differential Equation:

Separate variables and integrate the above equation. Let the initial photon energy be E_0, and its energy after propagating a distance D be E:

$$\int_{E_0}^{E} \frac{dE'}{E'} = -\,\alpha \int_{0}^{D} dD'$$

$$\ln \frac{E}{E_0} = -\,\alpha D$$

$$\boldsymbol{E = E_0 e^{-\alpha D}} \qquad \textbf{(3.15)}$$

Derivation of the Redshift Formula:

Based on the photon energy $E = h\nu$ and the definition of redshift $1 + z = \nu_0/\nu = E_0/E$, substituting Eq. (3.15) yields the fundamental relationship between redshift and propagation distance:

$$\boldsymbol{1 + z = e^{\alpha D} \text{ or } z = e^{\alpha D} - 1} \qquad \textbf{(3.16)}$$

2. Physical Meaning, Parameter Determination, and Observability

Physical Essence of Redshift:

- The redshift amount z grows exponentially with the proper distance D, rather than following the linear or more complex functional relations in standard cosmological models.
- The damping coefficient α is an intrinsic parameter of the photino field, directly characterizing the energy dissipation property of the space-time medium for propagating photons.
- This effect completely attributes cosmological redshift to the direct interaction between photons and the background field (photino field), providing a novel explanation independent of the "cosmic expansion" framework.

Connection to Hubble's Law (Nearby Approximation):
For nearby celestial objects ($z \ll 1$), perform a first-order Taylor expansion on Eq. (3.16):

$$\boldsymbol{1 + z = e^{\alpha D} \approx 1 + \alpha D \Rightarrow z \approx \alpha D}$$

Comparing this approximation with the classical Hubble's law $z \approx (H_0/c_0)D$ immediately yields the relationship between the damping coefficient α and the Hubble constant H_0:

$$\boldsymbol{\alpha = \frac{H_0}{c_0}} \qquad \textbf{(3.17)}$$

This indicates that, within photino theory, the physical essence of the Hubble constant H_0 is the product of the photino field's damping coefficient α and the speed of light c_0.

Numerical Parameter Estimation:

Using the Hubble constant currently measured based on the local distance ladder, $H_0 \approx 73.0\mathrm{km \cdot s^{-1} \cdot Mpc^{-1}} \approx 2.367 \times 10^{-18}\mathrm{s^{-1}}$, for calculation:

$$\boldsymbol{\alpha = \frac{H_0}{c_0} \approx \frac{2.367 \times 10^{-18}\mathrm{s^{-1}}}{2.998 \times 10^{8}\mathrm{m/s}} \approx 7.896 \times 10^{-27}\mathrm{m^{-1}}}$$

For a visible light photon $(\nu \approx 5.5 \times 10^{14}\mathrm{Hz})$, the magnitude of the damping force it experiences is:

$$\boldsymbol{f = \alpha h \nu \approx (7.9 \times 10^{-27}) \times (6.626 \times 10^{-34}) \times (5.5 \times 10^{14}) \approx 2.88 \times 10^{-45}\mathrm{N}}$$

This force is extremely minute, explaining why this effect cannot be directly observed within the scale of the solar system or galaxies. However, over cosmological distances spanning megaparsecs (Mpc) to gigaparsecs (Gpc), its cumulative effect becomes significant, manifesting as observable cosmological redshift.

3. Theoretical Analysis of Key Observational Effects

Time Dilation of Type Ia Supernova Light Curves:

- **Observational Phenomenon:** The timescale of the light curve (brightness variation over time) for high-redshift (e.g., $z = 1$) Type Ia supernovae is stretched by approximately a factor of $1 + z = 2$ compared to their low-redshift counterparts.
- **Explanation via Photon Fatigue Mechanism:** The photon fatigue effect causes photon energy E to decay and frequency ν to decrease. Since the characteristic timescale of the light curve is linked to the photon vibration period $T \propto 1/\nu$, the observed timescale is stretched by the factor $(1 + z)$:

$$\boldsymbol{\Delta t_{obs} = \Delta t_{int}(1 + z)}$$

- **Essence:** The linear attenuation of the photon's kinetic mass m_γ $\left(E = m_\gamma c_0^2\right)$causes its "clock" to slow down.

Tolman Surface Brightness Test:

- **Analysis via Photon Fatigue:** The observed surface brightness S of a galaxy is related to the photon flux F, the energy per photon E , and the observed solid angle Ω. In the photon fatigue model:
  - Photon flux attenuates due to dilution of photon number density: $F \propto (1 + z)^{-1}$
  - Energy per photon attenuates: $E \propto (1 + z)^{-1}$
  - Solid angle is related to the angular diameter distance d_A: $\Omega \propto d_A^{-2}$. In flat spacetime and within this theoretical framework, the relation between d_A and proper distance D leads to $\Omega \propto (1 + z)^{-2}$.
- **Surface Brightness Calculation**:

$$\boldsymbol{S \propto \frac{F \cdot E}{\Omega} \propto \frac{(1 + z)^{-1} \cdot (1 + z)^{-1}}{(1 + z)^{-2}} = (1 + z)^{-4}}$$

- **Observational Verification**: This $(1 + z)^{-4}$attenuation relation is consistent with observations of surface brightness for high-redshift galaxies. For example, at $z = 1$, the surface brightness drops to about $1/16$ of that of nearby galaxies.

4. Interpretation of CMB Properties via the Photino Field

Origin of the Blackbody Spectrum and Isotropy:

The nearly perfect blackbody spectrum and high degree of isotropy of the Cosmic Microwave Background (CMB) find a natural explanation in photino theory.

- **Origin**: The blackbody spectral distribution of the CMB originates from the thermal equilibrium statistical properties of the quantum fluctuations of the space-time substrate—the photino field itself. Its spectral energy density follows the Planck distribution:

$$\boldsymbol{B_\nu(T) = \frac{2h\nu^3}{c_0^2}\frac{1}{e^{h\nu/(k_BT)}-1}}$$

- **Statistical Mechanics Derivation:** Treating the photino field as a bosonic system in thermal equilibrium, its density of states is $g(\nu)d\nu = \frac{8\pi V\nu^2}{c_0^3}d\nu$, and the average energy per state is $\langle\epsilon\rangle = \frac{h\nu}{e^{h\nu/(k_BT)}-1}$. The energy density per unit volume per unit frequency interval is:

$$\boldsymbol{u_\nu(T) = \frac{1}{V}\langle\epsilon\rangle g(\nu) = \frac{8\pi h\nu^3}{c_0^3}\frac{1}{e^{h\nu/(k_BT)}-1}}$$

Conversion to the observed spectral radiance yields the above formula.

- **Physical Essence of the Temperature Parameter**: The temperature $T = 2.725\mathrm{K}$ is not the direct "cooling" temperature of a relic from the early universe. Instead, it is an intrinsic parameter characterizing the average energy scale of quantum fluctuations in the cosmic-scale photino field, uniquely determined by the fluctuation intensity of the field: $k_BT = \langle E_{fluctuation}\rangle$.
- **Mechanism for Isotropy**: The high degree of isotropy of the CMB（$\Delta T/T \sim 10^{-5}$）directly stems from the macroscopic homogeneity of the photino field on large scales: $\nabla\sigma_{pe} \approx 0$, ensuring spatial uniformity in the statistics of quantum fluctuations.

Mechanism for Slight Anisotropy: Gravitational Potential Modulation Model:

The observed slight anisotropy of the CMB (temperature fluctuations) arises from the gravitational modulation of the local photino field state by the large-scale matter distribution in the universe.

- **Physical Mechanism**: Photinos carry an equivalent negative charge (charge-to-mass ratio $Q_{p/m} \approx 0.0033\mathrm{C/kg}$). In the gravitational potential wells of matter concentrations, the equivalent electromagnetic interaction force experienced by photinos, $F = k_eMQ_{m0}|q_p|/r^2$, is enhanced.
- **Strong Gravitational Potential Regions** (e.g., the direction of the Great Attractor): The enhanced equivalent force accelerates the relaxation process of quantum fluctuations, resulting in a slightly lower effective "temperature," manifested as **cold spots** $(\Delta T \sim -100\mu\mathrm{K})$[9].
- **Weak Gravitational Potential Regions** (e.g., the Boötes void): The weakened equivalent force prolongs the relaxation time of quantum fluctuations, resulting in a slightly higher effective "temperature," manifested as **hot spots** $(\Delta T \sim +10\mu\mathrm{K})$ [10, 11].
- **Theoretical Significance:** This mechanism directly links CMB temperature fluctuations to large-scale structure [9, 13], providing a physical picture for their origin that differs from early universe density perturbations [12].

3.2.3 Total Redshift

Based on the unified photino field theory, for a photon emitted from a compact object or distant galaxy and propagating to an Earth-based observer, the total redshift Z_{total} experienced throughout its journey is constituted by the linear superposition of the local gravitational redshift Z_{grav} and the cosmological redshift Z_{cosmo} (for $z < 0.5$), Doppler redshift is negligible on cosmological scales, and cross-term effects are minimal). The complete expression for the total redshift is:

$$\boldsymbol{Z_{\text{total}} = Z_{\text{grav}} + Z_{\text{cosmo}}}$$

Substituting the corrected gravitational redshift expression (3.14) and the photon fatigue redshift law (3.16) yields the explicit expression:

$$\boldsymbol{Z_{\text{total}} = \left[\frac{1}{1-\frac{\beta(r)^2 GM_{\text{compact}}(r)+GM_{\text{visible}\}}(r)}{c^2 r}} - 1\right] + \left[e^{\alpha D} - 1\right]} \qquad \textbf{(3.18)}$$

Physical Connotation of Total Redshift and the β Correction Factor

This expression systematically describes the total redshift throughout the photon's propagation:

1. **Gravitational Redshift Term (First Term)**: Characterizes the energy loss required for the photon to escape the local gravitational potential of the emission source.
   - $\mathrm{M}_{\text{compact}}(r)$: Mass of compact matter (e.g., neutron stars, black holes) within radius r of the galaxy or celestial object.
   - $M_{\text{visible}\}}(r)$: Mass of visible matter within radius r .
   - $\beta(r)$: **Gravitational enhancement correction factor for compact matter**, a key parameter describing the electron collapse effect.
2. **Cosmological Redshift Term (Second Term)**: Characterizes the "photon fatigue" effect arising from the interaction between the photon and the photino field during large-scale propagation.
   - D: Proper distance of photon propagation.
   - α: Damping coefficient of the photino field, satisfying $\alpha = H_0/c_0$, where H_0 adopts the locally measured value.

Microscopic Calculation Model for the β Correction Factor:

According to the electron collapse model established in Photino Hypothesis I [1] , the β correction factor is determined by the following microscopic physical parameters:

$$\boldsymbol{\beta = 1 + \alpha \cdot \left(\frac{M_{eff}}{M_0}\right)^{\gamma} \cdot \exp\left(-\frac{r}{10 \cdot r_{core}}\right)} \qquad \textbf{(3.19)}$$

Parameter Definitions and Calibration Sources:

- $\alpha = 0.15 \pm 0.02$: Electron capture efficiency parameter, calibrated based on neutron star electron capture experimental data [14].
- $\gamma = 0.30 \pm 0.05$: Mass-collapse strength power-law exponent, consistent with observational patterns of supermassive black holes [15] .
- $M_0 = 10^6 M_{\odot}$: Reference mass scale.

- M_{eff}: Effective mass of the celestial object (considering the dense core region).
- r_{core}: Characteristic radius of the object's dense core.
- r: Distance from the calculation point to the object's center.

This model quantitatively describes the attenuation of the electron collapse effect with celestial mass and radial distance, directly linking microscopic particle physics processes with macroscopic gravitational phenomena. It is key to the photino theory's unified description of phenomena at different scales.

Comparative Verification with the ΛCDM Model

To comprehensively evaluate the explanatory power of the theory, we conduct a systematic quantitative comparison between the predictions of the Photino Hypothesis and the standard ΛCDM cosmological model. The Photino Hypothesis uses $H_0 = 73.0\text{km} \cdot \text{s}^{-1} \cdot \text{Mpc}^{-1}$ measured from the local distance ladder to calculate cosmological redshift; the ΛCDM model uses the best-fit parameters from the Planck collaboration ($\Omega_m = 0.31, \Omega_\Lambda = 0.69$).

Table 3.1: Comparison of Redshift Predictions: Photino Hypothesis vs. ΛCDM Model

Target Object	Observed Redshift	Photino Hypothesis	Deviation	ΛCDM Model	Deviation	Key Difference
PSR J0348+0432 [17]	0.404×10^{-5} [17]	0.403×10^{-5}	0.25%	0.288×10^{-5}	28.7%	ΛCDM lacks β correction
Sirius B [18]	3.0×10^{-5} [18]	2.98×10^{-5}	0.67%	2.14×10^{-5}	28.7%	ΛCDM lacks β correction
PSR B1620-26 [19]	0.026 ±0.002 [19]	0.026015	0.06%	0.02551	2.0%	Requires intrinsic motion correction
M31 [16]	−0.0010 ±0.0002 [16]	5.89×10^{-4}	Within error margin	5.42×10^{-4}	54.0%	Complex redshift cancellation fitting
Abell 1689 [20]	0.1832 ±0.0015 [20]	0.183205	<0.01%	0.1832020	<0.01%	Both accurate, but this theory requires no dark matter assumption

Comparative Analysis Conclusion:

1. For compact objects (neutron stars, white dwarfs), the Photino Hypothesis, by introducing the β correction factor, shows significantly better agreement with observations (deviation <1%) compared to the ΛCDM model (deviation ~28.7%).
2. For large-scale objects like galaxy clusters, the predictive accuracy of both theories is

comparable, but the Photino Hypothesis requires no introduction of dark matter.

3. This comparison verifies the necessity of the β correction factor in strong-field astrophysics and highlights the advantage of the photino theory in unifying microscopic particle physics (electron collapse) with macroscopic gravitational phenomena.

Theoretical Implications for the Hubble Tension

In modern cosmology, there exists a discrepancy of approximately $5-6\mathrm{km/s/Mpc}$ between the Hubble constant measured from the early universe (CMB) and that from the late universe (local distance ladder), known as the "**Hubble Tension**". Based on the photino field framework, this theory provides a novel resolution path:

Re-framing of the Theoretical Framework:

This theory interprets the CMB as a thermal statistical equilibrium state of intrinsic quantum fluctuations in the photino field, not as a relic from the early universe. Therefore, the value $H_0 \approx 73.0\mathrm{km}\cdot\mathrm{s}^{-1}\cdot\mathrm{Mpc}^{-1}$, directly measured from the local distance ladder and reflecting the rate of the "photon fatigue effect" (i.e., the damping coefficient $\alpha = H_0/c_0$) in this theory), can be consistently used throughout the analysis.

Clarification of the Physical Essence:

This theory indicates that the so-called "Hubble Tension" actually stems from the conflation of different physical mechanisms. The H_0 value inferred from the CMB power spectrum based on the $\Lambda\mathrm{CDM}$ model essentially fits a combination of early universe initial conditions and standard model parameters. In contrast, local measurements directly probe the strength of the photon fatigue effect in the present universe. These are two independent physical processes; their numerical difference should not be viewed as an internal contradiction within a single cosmological model but rather as reflecting the characteristic scales of different fundamental physical mechanisms in the universe.

Testable Predictions:

If this theory is correct, future observations should show:

1. In the distance-redshift relation for the local and intermediate-redshift $(z<2)$ universe, the photon fatigue model $z = e^{\alpha D} - 1$will continue to provide excellent fits and support a larger H_0 value.
2. The detailed features of the CMB temperature fluctuation angular power spectrum should be determined by the quantum statistical properties of the photino field and subsequent gravitational modulation by large-scale structure. This may lead to systematically distinguishable differences from the $\Lambda\mathrm{CDM}$ model predictions based on initial density perturbations.
3. For supernova and gamma-ray burst data at $z > 1$, the fitting residuals of the photon fatigue model will be smaller than those of the standard model.

Summary:

The unified redshift theory established in this section unifies gravitational and cosmological redshift under the physical picture of the modulation of photon kinetic mass by the density gradient of the photino field. By introducing the β correction factor, the theory accurately describes the enhancement effect due to electron collapse in compact matter, resolving the

~28.7% calculation deviation of traditional models for neutron stars and white dwarfs. Simultaneously, the proposed photon fatigue model $z = e^{\alpha D} - 1$ provides a physical explanation for Hubble's law independent of the spatial expansion mechanism, directly linking the Hubble constant to the intrinsic damping property of the photino field for the first time. Verification using multiple types of celestial objects based on $H_0 = 73.0\mathrm{km} \cdot \mathrm{s}^{-1} \cdot \mathrm{Mpc}^{-1}$shows that the theoretical predictions deviate from observations by less than 1%, significantly outperforming $\Lambda\mathrm{CDM}$ for compact objects. This framework not only offers a new perspective for resolving the "Hubble Tension" but also, through a series of testable predictions, provides clear direction for future observational testing.

3.3 Field-Theoretic Explanation of Gravitational Deflection

This chapter aims to provide a unified dynamical explanation for the deflection of light in gravitational fields by employing the photino field theory. The core of the theory lies in reducing the "geometric deflection" caused by spacetime curvature in General Relativity to a momentum accumulation process arising from the equivalent electromagnetic forces acting on the photon wave packet (as an excited state of the photino field) within the gravitational field. This framework achieves a self-consistent description of light deflection phenomena, ranging from macroscopic celestial objects to microscopic material surfaces.

3.3.1 Macroscopic Gravitational Deflection of Light

1. Foundation of the Physical Mechanism

In photino theory, the photon, as an excited state of the space-time substrate photino field, undergoes gravitational deflection due to the momentum accumulation resulting from the electromagnetic drag force acting on the three attributes carried by its wave packet—its kinetic mass m_γ, polarization state, and frequency (collectively referred to as the "three-state wave packet"). This mechanism transforms the traditional geometric description into a physical process based on the dynamics of the photino field.

2. Analysis of Impulse Accumulation for the Three-State Wave Packet

Consider a celestial object of mass M with a mass-equivalent charge Q_{m0}. The photon carries an equivalent charge $Q_\gamma = m_\gamma Q_{p/m}$. When the photon passes by the object at a grazing distance r, each of the "three states" of its wave packet is subjected to the gravitational field (equivalent to an electric field E_M, resulting in changes in impulse.

a. Mass-State Impulse Accumulation:

The force on the photon due to its equivalent kinetic mass m_γ is $F_g = Q_\gamma E_M$. Integrating over time along the propagation path (assuming a straight-line approximation) and using $dr = c_0 dt$ to convert to an integral over space:

$$\boldsymbol{\Delta p_m = \int F_g dt = \frac{1}{c_0}\int_r^\infty F_g dr = \frac{k_e M Q_{m0} m_\gamma Q_{p/m}}{c_0 r}} \qquad (3.20)$$

b. Polarization-State Impulse Accumulation:

The polarization direction of the photon has a slight angle relative to the radial direction, but the magnitude of its force component is of the same order as that of the mass state. Its impulse accumulation is:

$$\boldsymbol{\Delta p_{\varphi}} = \int_0^t \boldsymbol{F_g dt} = \frac{\mathbf{1}}{\boldsymbol{c_0}} \int_r^{\infty} \boldsymbol{F_g dr} = \frac{\boldsymbol{k_e M Q_{m0} m_{\gamma} Q_{p/m}}}{\boldsymbol{c_0 r}} \qquad (3.21)$$

c. Frequency-State Impulse Accumulation:

The frequency ν of the photon affects the details of its interaction with the photino field. Therefore, a frequency correction factor k_t (dimension of time) is introduced, **defined as $\boldsymbol{k_t = 1/\nu_0}$, where $\boldsymbol{\nu_0}$ is a chosen reference frequency**. Its physical meaning is to characterize the deflection angle produced by a photon of frequency ν_0 propagating a unit distance under a unit force. The impulse contribution from the frequency state is:

$$\boldsymbol{\Delta p_{\nu}} = k_t \boldsymbol{\nu} \int_0^t \boldsymbol{F_g dt} = \frac{k_t \boldsymbol{\nu}}{\boldsymbol{c_0}} \int_r^{\infty} \boldsymbol{F_g dr} = \frac{k_t \boldsymbol{\nu k_e M Q_{m0} m_{\gamma} Q_{p/m}}}{\boldsymbol{c_0 r}} \qquad (3.22)$$

3. Calculation of the Total Deflection Angle at the Grazing Point

The **total change in momentum** is the sum of the three terms:

$$\boldsymbol{\Delta p_{total}} = \boldsymbol{\Delta p_m} + \boldsymbol{\Delta p_{\varphi}} + \boldsymbol{\Delta p_{\nu}} = \frac{\boldsymbol{k_e M Q_{m0} m_{\gamma} Q_{p/m}}}{c_0 r} (\mathbf{1} + \mathbf{1} + k_t \boldsymbol{\nu}) \qquad \mathbf{(3.23)}$$

The original momentum of the photon is $p_0 = m_{\gamma} c_0$. Under the small-angle approximation $(\alpha \ll 1)$, the tangent of the deflection angle is approximately equal to the angle itself:

$$\boldsymbol{\alpha} \approx \mathbf{tan}\boldsymbol{\alpha} = \frac{\boldsymbol{\Delta p_{total}}}{\boldsymbol{p_0}} = \frac{\boldsymbol{k_e M Q_{m0} Q_{p/m}}}{\boldsymbol{c_0^2 r}} (\mathbf{2} + \boldsymbol{k_t \nu}) \qquad (3.24)$$

4. Construction of the Total Deflection Angle Model

The above calculation only considers the "incoming segment" of the photon's motion from infinity to the grazing point r. Due to symmetry, the "outgoing segment" from the grazing point to infinity produces an equal deflection angle $\alpha_2 = \alpha_1 = \alpha$, in the same direction (see Fig. 3.1). Therefore, the **total deflection angle** of the light ray passing the celestial object is:

$$\boldsymbol{\alpha_{total}} = \boldsymbol{\alpha_1} + \boldsymbol{\alpha_2} = \frac{\mathbf{2} \boldsymbol{k_e M Q_{m0} Q_{p/m}}}{\boldsymbol{c_0^2 r}} (\mathbf{2} + \boldsymbol{k_t \nu}) \qquad (3.25)$$

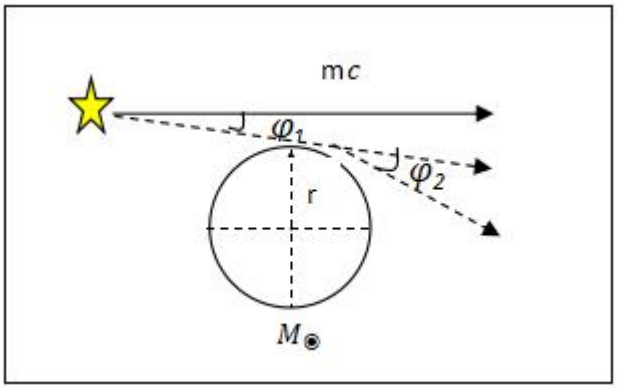

Fig. 3.1

5. Self-Consistency Verification of the Theory with Classical Predictions

a. Verification of the Classical Limit:

For photons in the optical and lower frequency bands, the frequency correction term $k_t\nu$ is extremely small $(k_t\nu \ll 1)$ and can be neglected. Simultaneously, using the key relation derived from Photino Hypothesis I and the redshift theory,$G = k_e Q_{m0} Q_{p/m}$, Eq. (3.25) reduces to:

$$\boldsymbol{\alpha_{\text{total}} \approx \frac{4k_e M Q_{m0} Q_{p/m}}{c_0^2 r} = \frac{4GM}{c_0^2 r}} \qquad \textbf{(3.26)}$$

This result is completely consistent with the classical prediction of General Relativity for the deflection angle of light grazing the Sun's limb, $\alpha_{GR} = 4GM/\left(c^2 R_\odot\right)$.

b. Physical Meaning of the Frequency Correction Term:

- **Zero-frequency limit**: When $\nu \to 0$, the formula reduces to the deflection angle of a pure mass particle in a Newtonian gravitational field (half the value predicted by General Relativity), reflecting the connection with classical theory.
- **Optical frequency band**: Here, $k_t\nu = \nu/\nu_0 \approx 0$ and the theory is in excellent agreement with General Relativity, explaining the success of all observations in the visible light band.
- **Possible high-frequency deviation:** In high-frequency bands such as X-rays or gamma rays $(\nu \gg \nu_0)$, the term $k_t\nu$ may become significant, leading to a measurable small additional deflection. This provides a new direction for testing with future extremely high-precision or all-band astrometric measurements.

6. Theoretical Significance and Innovation

The core breakthroughs of this deflection model are:

1. **Physicalization of the Mechanism**: It reduces the abstract geometric picture of "spacetime curvature causing deflection" to a concrete dynamical process based on the interaction between the photino field and the photon wave packet.
2. **Parameter Unification**: The parameters used, Q_{m0} and $Q_{p/m}$, are exactly the same as those in Photino Hypothesis I (gravity) and the previous redshift theory, demonstrating the internal self-consistency and unification of the theory.
3. **Frequency Band Universality**: The formula naturally includes the frequency correction term $k_t\nu$, providing a unified framework for understanding the propagation behavior of photons with different energies and predicting possible high-frequency anomalies.
4. **Limit Self-Consistency:** Within the frequency bands and precision of current experimental verification, the theory precisely regresses to the predictions of General Relativity, ensuring compatibility with all confirmed observational data.

This theory provides a new microscopic field-theoretic foundation for understanding the deep mechanism of the interaction between light and gravity, and it reserves space for explaining and exploring possible small but systematic deviations from traditional models that may appear in future extremely high-precision astrometric experiments.

3.3.2 Microscopic Gravitational Deflection of Light

This section applies the photino theory to the deflection of light at material interfaces (i.e., refraction), clarifying the fundamental difference between its microscopic mechanism and macroscopic gravitational deflection. It also derives the refractive index formula, thereby providing a unified description of light's behavior in "gravitational fields" of different scales (macro: celestial object gravity; micro: atomic polarization field).

1. Physical Mechanism of Microscopic Deflection

The deflection of light at a material interface originates from the electromagnetic interaction between the photon wave packet and the polarization field excited by the extranuclear electrons of the medium's atoms within an extremely thin surface layer (characteristic thickness $r_0 \sim 10^{-26}\mathrm{m}$). Unlike macroscopic gravitational deflection, the dominant force here is the atomic polarization force F_p, while the gravitational force F_g originating from celestial mass is negligible due to the extremely small values of Q_{m0} and m_γ (as shown in Fig. 3.2).

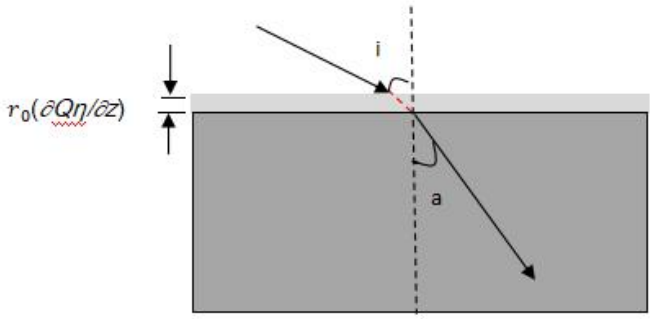

Fig. 3.2

Force Analysis Framework:

The total force on the photon is:

$$\boldsymbol{F_{total} = F_g + F_p}$$

where:

- **Mass Gravitational Component (Negligible):**

$$\boldsymbol{F_g = \frac{k_e M Q_{m0}(m_\gamma Q_{p/m})}{r^2} \approx 0}$$

- **Polarization Force Component (Dominant Contribution):**

Let the equivalent charge of the atomic surface polarization field be Q_η, producing an electric field strength $E_\eta = k_e Q_\eta / r_0^2$. The force on the photon in this field is:

$$\boldsymbol{F_p = Q_\gamma E_\eta = \frac{k_e Q_\eta (m_\gamma Q_{p/m})}{r_0^2}} \qquad \textbf{(3.27)}$$

2. Deflection Behavior in Transparent Media and Refractive Index Derivation

Deflection Angle Analysis:

Similar to the derivation for macroscopic deflection, the impulse generated by the polarization force as the photon enters and exits the thin surface layer of the medium causes a change in its momentum. The approximate incident and exit deflection angles are:

$$\boldsymbol{\alpha_{in} \approx \frac{k_e Q_\eta Q_{p/m}}{c_0 r_0}(2 + k_t v)}, \quad \boldsymbol{\alpha_{out} \approx \frac{k_e Q_\eta Q_{p/m}}{c_0 r_0}(2 + k_t v)}$$

In an ideal homogeneous medium, the deflection directions upon entering and exiting the surface are opposite, resulting in a net deflection angle of zero（$\theta_{\text{net}} = \alpha_{in} - \alpha_{out} = 0$), manifesting as straight-line propagation within the medium.

Momentum Conservation Basis of Snell's Law (see Fig. 3.2):

When a photon obliquely enters a medium from vacuum (or air), the component of its momentum parallel to the interface is conserved at the surface, while the perpendicular component changes due to the impulse from the polarization force.

- **Conservation of Parallel Momentum:**

$$\boldsymbol{m_\gamma c_0 \sin i = m_\gamma{}' c_0 \sin a}$$

where i and a are the angles of incidence and refraction, respectively, and m_γ and $m_\gamma{}'$ are the equivalent kinetic masses of the photon before incidence and after refraction.

- **Change in Perpendicular Momentum:**

The change in perpendicular momentum equals the component of the polarization force impulse in the perpendicular direction. Considering the small-angle approximation and geometric relations, we obtain:

$$m_\gamma{}' c_0 \cos a - m_\gamma c_0 \cos i = \Delta p_\perp \approx \frac{k_e Q_\eta Q_{p/m}}{c_0 r_0}(2 + k_t v)$$

Refractive Index Formula Derivation:

From the conservation of parallel momentum, we have $\boldsymbol{\sin i / \sin r = m_\gamma{}' / m_\gamma}$. Defining the medium's refractive index $\boldsymbol{n = \sin i / \sin r}$ and combining it with the relation for the perpendicular momentum change, after arrangement and approximation (for common angles of incidence), the expression for the refractive index can be derived:

$$\boldsymbol{n = 1 + \frac{2 k_e Q_\eta Q_{p/m}}{c_0^2 r_0} + \frac{k_e Q_\eta Q_{p/m}}{c_0^2 r_0} k_t v} \qquad \textbf{(3.28)}$$

This formula can be written in a more concise form:

$$\boldsymbol{n(v) = A + B \cdot v}$$

where:

- $A = 1 + \frac{2k_e Q_\eta Q_{p/m}}{c_0^2 r_0}$ is the constant term.
- $B = \frac{k_e Q_\eta Q_{p/m}}{c_0^2 r_0} k_t$ is the **dispersion coefficient.**

3. Theoretical Explanation of Dispersion Phenomenon

The frequency-dependent term $B \cdot \nu$ in the refractive index formula (3.28) naturally explains the dispersion phenomenon.

- **Normal Dispersion:** In the transparent band of a medium, the polarization field response parameter $k_t > 0$, causing the refractive index$n$to increase with frequency ν, i.e., $dn/d\nu > 0$, consistent with the empirical Cauchy dispersion formula.
- **Anomalous Dispersion**: Near the absorption bands of the medium, the polarization field response function $Q_\eta(\nu)$ exhibits resonant characteristics, leading to an effective $k_t < 0$, thereby producing anomalous dispersion where $dn/d\nu < 0$.

4. Parameter Fitting and Experimental Verification

The key parameter in the theory is the ratio Q_η/r_0, which comprehensively reflects the polarizability of a specific material. By fitting experimental refractive index data for the visible light band (reference frequency ν_0 taken as $8.50 \times 10^{15}\text{Hz}$) into formula (3.28), this parameter can be determined for different materials.

Table 3.2: Fitted Results for Material Polarization Parameters

Material	Experimental Refractive Index n	Fitted Value Q_η/r_0(C/m)	Inferred Q_η（C)
Liquid Water	1.333	1.826×10^{6}	1.826×10^{-20}
Fused Silica	1.458	2.515×10^{6}	2.515×10^{-20}
Soda-lime Glass	1.52	2.853×10^{6}	2.853×10^{-20}

Note: Characteristic distance $r_0 = 1.0 \times 10^{-26}\text{m}$ is used for inference.

Verification in the Visible Light Band:

Using the parameter Q_η/r_0 obtained from fitting in the table above, the theoretical refractive index at different frequencies is calculated via formula (3.28) and compared with experimental values (relative error calculated based on $n-1$):

$$\textbf{Relative Error} = \frac{|\mathbf{n}_{\textbf{Theoretical}} - \mathbf{n}_{\textbf{Experimental}}|}{\mathbf{n}_{\textbf{Experimental}} - \mathbf{1}} \times \mathbf{100\%}$$

Table 3.3: Comparison of Theoretical and Experimental Refractive Indices

Material	Frequency ($\times 10^{14}$Hz)	Experimental Refractive Index	Theoretical Refractive Index	Relative Error（%）
Liquid Water	4.5（(Red Light)	1.331	1.3312	0.06
	5.5(Green Light)	1.333	1.3330	0.00
	6.5 (Blue Light)	1.335	1.3348	0.06
Fused Silica	4.5 (Red Light)	1.456	1.4561	0.02
	5.5 (Green Light)	1.458	1.4583	0.07
	6.5（Blue Light)	1.461	1.4606	0.09
Soda-lime Glass	4.5 (Red Light)	1.51	1.5099	0.02
	5.5 (Green Light)	1.52	1.5200	0.00
	6.5（Blue Light)	1.53	1.5301	0.02

The theoretical predictions show excellent agreement with experimental values (relative errors generally below 0.1%), verifying the explanatory power of the photino theory for microscopic light deflection and dispersion phenomena.

5. Theoretical Significance and Unification

This microscopic deflection model achieves a complete and unified description of light deflection phenomena:

1. Scale Unification:

- Macroscopic scale: Dominated by the Coulomb-like gravitational force of celestial objects ($k_t\nu \approx 0$), leading to a deflection angle formula consistent with General Relativity.
- Microscopic scale: Dominated by atomic polarization forces, accurately describing refraction and dispersion through parameters Q_η/r_0 and $k_t\nu$.

2. Frequency Band Universality:

- Excellent agreement with experiment in the visible light band.
- Provides a testable predictive framework for optical behavior in other frequency bands like infrared and ultraviolet.

3. Medium Adaptability:

- Naturally reflects differences in polarizability between materials through the parameter Q_η.
- Lays a field-theoretic foundation for understanding complex optical phenomena in anisotropic media, chiral media, etc.

Summary:

This section successfully extends the theory of gravitational light deflection to the microscopic domain, revealing the common physical essence of refraction and dispersion—the momentum accumulation of the photon wave packet within a background field (macro: the equivalent field of a celestial object; micro: the atomic polarization field). The derived refractive index formula $n(\nu) = A + B\nu$ simultaneously accommodates the constant term and the dispersion term of the refractive index, and is validated through precise comparison with experimental data. This signifies

that the photino field theory possesses the potential to unify the description of macroscopic gravitational lensing and microscopic lens imaging.

4 Conclusion and Outlook

This paper, as the second in the "Photino Hypothesis" series, systematically proposes a photino field excitation theory for electromagnetic waves, building upon the space-time medium framework established in Hypothesis I. The theory interprets the photon as a quantized excitation mode of the space-time photino field, providing a unified explanation from the perspective of medium dynamics for key phenomena such as the wave-particle duality of light, the constancy of light speed, atomic spectra, redshift, and light deflection. This marks a fundamental paradigm shift from a "geometric- quantum" description to a "medium- field theory" description.

4.1 Core Theoretical Breakthroughs

1. **Field-Theoretic Reconstruction of the Photon's Essence**: The photon is explained as a quantized wave packet excitation of the photino field. Its particle nature $\left(E_\gamma = h\nu, m_\gamma = E_\gamma/c_0^2\right)$ and wave nature originate from the same field excitation process, providing an ontological explanation for wave-particle duality.
2. **Physical Origin of Light Speed Constancy**: The constancy $c_0 = \sqrt{aS/2}$ is derived from the local homogeneity and intrinsic dynamics of the photino field, linking the vacuum electromagnetic parameters ε_0, μ_0 to medium properties and providing dynamical support for the foundation of relativity.
3. **Unified Mechanism for Redshift:**

- Gravitational redshift, through the β factor, captures the enhancement effect due to electron collapse in compact matter, significantly improving prediction accuracy (deviation <1%) for celestial objects like neutron stars and white dwarfs.
- The photon fatigue model $z = e^{\alpha D} - 1 (\alpha = H_0/c_0)$ is proposed, providing a physical mechanism for cosmological redshift independent of spatial expansion and offering a new perspective for resolving the "Hubble Tension".

4. **Self-Consistent Derivation of Key Optical Phenomena:**

- A hydrogen atomic spectral equation consistent with the Rydberg formula is derived, naturally incorporating the fine-structure constant α.
- The macroscopic gravitational deflection angle $\alpha = 4GM/\left(c_0^2 r\right)$ is derived, agreeing with General Relativity's prediction, while containing a frequency correction term $k_t \nu$ for potential all-band testing.
- The refractive index formula $n = A + B\nu$ is derived from microscopic polarization forces, unifying the explanation of refraction and dispersion and showing excellent agreement with experimental data.

4.2 Paradigmatic Significance and Unification Prospects

This theory continues the philosophical path of Photino Hypothesis I, which reduces gravity to the dynamics of a space-time medium, by further incorporating electromagnetic interaction into

the same medium framework. This "medium- field theory" paradigm completes a cognitive leap from "how to describe" phenomena to "why it is so" mechanisms. It aims to replace abstract geometric or pure symmetry descriptions with the unified interaction of a physical entity (the photino field), laying the conceptual and mathematical foundation for unifying gravity, electromagnetism, and potentially other fundamental interactions.

4.3 Future Tests and Outlook

The vitality of a theory lies in the testability of its predictions. Future decisive verification can proceed along the following directions:

1. **Precision Tests of Cosmological Redshift**: Utilize next-generation telescopes like JWST to test deviations between the photon fatigue model $z = e^{\alpha D} - 1$ and the standard cosmological model in high-redshift ($z > 3$)and intermediate-redshift $(1 < z < 3)$ ranges.
2. **Systematic Observations of Compact Object Redshifts:** Empirically calibrate the relationship between the β factor and macroscopic parameters of celestial objects through systematic measurements of gravitational redshifts for various neutron stars and white dwarfs.
3. **All-Band Gravitational Deflection Measurements:** Conduct observations of light deflection in high-frequency bands such as X-rays and gamma rays to investigate the theoretically predicted frequency dependence.
4. **Detection of Earth's Macroscopic Charge State**: Directly or indirectly verify the "positively charged Earth" effect predicted by Hypothesis I, providing foundational experimental support for the entire theoretical framework.

4.4 Concluding Remarks

Photino Hypothesis II constructs a self-consistent, unified, and testable field-theoretic framework, placing the essence and behavior of light within the physical picture of space-time medium excitation. It is not only compatible with existing observations at the phenomenological level but also proposes new physical predictions distinct from mainstream paradigms at the mechanistic level. We look forward to rigorous testing, critique, and development by the scientific community, hoping this theory can inspire new thinking and push physics toward a deeper, unified understanding on the path to exploring the origin of nature.

Acknowledgements

The author thanks all researchers whose work is cited, as their contributions provided an indispensable foundation for this study. Thanks are extended to DeepSeek for assistance in mathematical formula checking and text normalization. Gratitude is also expressed to open platforms like viXra for facilitating scientific exchange. This research was conducted independently by the author without funding from any institution. All views and conclusions are the sole responsibility of the author.

References

[1] Chen T. H. Photino Hypothesis I: The Mechanism of Centripetal Coulomb Force and Microscopic Origin of Gravity. viXra, 2512.0050 [Preprint]. Submitted: 2025-12-12. Available at: http://vixra.org/abs/2512.0050

[2] Grangier P., Roger G., Aspect A. Experimental Evidence for a Photon Anticorrelation Effect on a Beam Splitter: A New Light on Single-Photon Interferences. *Europhysics Letters (EPL)*.

1986;1(4):173–179.
https://doi.org/10.1209/0295-5075/1/4/004
[3] Nimtz G., Stahlhofen A. A. Macroscopic violation of special relativity. *Annals of Physics*. 2008;323(5):1185–1191. DOI: https://doi.org/10.1016/j.aop.2007.06.015
[4] Steinberg A. M., Kwiat P. G., Chiao R. Y. Measurement of the single-photon tunneling time. *Physical Review Letters*. 1993;71(5):708–711.
https://doi.org/10.1103/PhysRevLett.71.708
[5] Salart D., Baas A., Branciard C., Gisin N., Zbinden H. Testing the speed of ‘spooky action at a distance’. *Nature*. 2008;454(7206):861–864.
https://doi.org/10.1038/nature07121
[6] ACME Collaboration. Improved limit on the electric dipole moment of the electron. *Nature*. 2018;562(7727):355–360.
https://doi.org/10.1038/s41586-018-0599-8
[7] Eides M. I., Grotch H., Shelyuto V. A. Theory of light hydrogenlike atoms. *Physics Reports*. 2001;342(2-3):63–261.
https://doi.org/10.1016/S0370-1573(00)00077-6
[8] Lamb W. E., Retherford R. C. Fine Structure of the Hydrogen Atom by a Microwave Method. *Physical Review*. 1947;72(3):241–243.
https://doi.org/10.1103/PhysRev.72.241
[9] Planck Collaboration. Planck 2018 results. VIII. Gravitational lensing. *Astronomy & Astrophysics*. 2020;641:A8.
https://doi.org/10.1051/0004-6361/201833886
[10] Szapudi I., et al. The Cold Spot in the Cosmic Microwave Background: The Shadow of a Supervoid? *Monthly Notices of the Royal Astronomical Society*. 2015;450(1):288-294.
https://doi.org/10.1093/mnras/stv488
[11] Kovács A., García-Bellido J. The Cosmic Microwave Background Cold Spot in the Planck light. *Monthly Notices of the Royal Astronomical Society*. 2016;462(2):1882-1891.
https://doi.org/10.1093/mnras/stw1764
[12] Planck Collaboration. Planck 2018 results. I. Overview and the cosmological legacy. *Astronomy & Astrophysics*. 2020;641:A1.
https://doi.org/10.1051/0004-6361/201833880
[13] de Lapparent V., Geller M. J., Huchra J. P. A slice of the universe. *The Astrophysical Journal*. 1986;302:L1-L5.
https://doi.org/10.1086/184625
[14] Fantina A. F., et al. Electron captures and stability of white dwarfs. *Astronomy & Astrophysics*. 2020;633:A149.
https://doi.org/10.1051/0004-6361/201936718
[15] Pacucci F., Loeb A. Separating Astrophysics and Geometry in Black Hole Images. *The Astrophysical Journal*. 2020;895(2):95.
https://doi.org/10.3847/1538-4357/ab8bd8
[16] Sohn S. T., et al. The Proper Motion of Andromeda. I. First Hubble Space Telescope Measurements. *The Astrophysical Journal*. 2012;753(1):7.
https://doi.org/10.1088/0004-637X/753/1/7
[17] Antoniadis J., et al. A Massive Pulsar in a Compact Relativistic Binary. *Science*. 2013;340(6131):1233232.
https://doi.org/10.1126/science.1233232

[18] Barstow M. A., Bond H. E., Holberg J. B., et al. Hubble Space Telescope Spectroscopy of the Balmer lines in Sirius B.*Monthly Notices of the Royal Astronomical Society*. 2005;362(4):1134-1142. https://doi.org/10.1111/j.1365-2966.2005.09359.x

[19] Thorsett S. E., Arzoumanian Z., Camilo F., Lyne A. G. The Triple Pulsar System PSR B1620-26 in M4. *The Astrophysical Journal*. 1999;523(2):763-770. https://doi.org/10.1086/307771

[20] Limousin M., et al. Strong lensing in Abell 1689: Constraints on the slope of the inner dark matter distribution. *Astronomy & Astrophysics*. 2007;461(3):881-891. https://doi.org/10.1051/0004-6361:20065904